European Commission

JRC TECHNICAL REPORTS

Results of average capture cross section measurements for ^{238}U at a 12 m and 60 m station of GELINA

Description of GELINA data to be stored in the EXFOR data base

Hyeong Il Kim
Carlos Paradela
Stefan Kopecky
Gery Alaerts
Andre Moens
Peter Schillebeeckx
Ruud Wynants

2016

Joint Research Centre

EUR 28347 EN

JRC Science Hub
https://ec.europa.eu/jrc

JRC104596

EUR 28347 EN

ISBN 978-92-79-64614-0

ISSN 1831-9424

doi:10.2789/34219

How to cite: H.I. Kim, C. Paradela, S. Kopecky, G. Alaerts, A. Moens, P. Schillebeeckx and R. Wynants; Results of average capture cross section measurements for ^{238}U at a 12 m and 60 m station of GELINA; EUR 28347 EN; doi:10.2789/34219

Results of average capture cross section measurements for ^{238}U at a 12 m and 60 m station of GELINA

H. I. Kim[a], C. Paradela[b], S. Kopecky[b], G. Alaerts[b], A. Moens[b], P. Schillebeeckx[b] and R. Wynants[b]

[a]Korea Atomic Energy Research Institute, Daejeon 34057, Republic of Korea

[b]European Commission, Joint Research Centre, B - 2440 Geel, Belgium

Contents

Abstract 6
1 Introduction 7
2 Experimental conditions 8
3 Data reduction 11
3.1 Experimental capture yield 11
3.2 Background for the flux measurements 11
3.3 Background for the capture measurements 12
3.4 Correction factor F_c 13
3.5 Normalization 14
3.6 Time–of–flight to energy conversion 14
4 Results 15
References 16
List of figures 18
List of tables 19
Appendix 20

Abstract

Measurements have been performed at the time-of-flight facility GELINA to determine the capture cross section for neutron induced reactions on ^{238}U. The measurements have been carried out at a 12 m and a 60 m capture station of GELINA with the accelerator operating at 800 Hz. This report provides the experimental details required to deliver the data to the EXFOR data library which is maintained by the Nuclear Data Section of the IAEA and the Nuclear Energy Agency of the OECD. The experimental conditions and data reduction procedures are described. In addition, the full covariance information based on the AGS concept is given such that nuclear reaction model parameters together with their covariances can be derived in a least squares adjustment to the data.

1 Introduction

To study the resonance structure of neutron induced reaction cross sections, neutron spectroscopic measurements are required which determine with a high accuracy the energy of the neutron that interacts with the material under investigation. To cover a broad energy range such measurements are best carried out with a pulsed white neutron source, which is optimized for time-of-flight (TOF) measurements [1].

The TOF-facility GELINA [2][3] has been designed and built for high-resolution cross section measurements in the resonance region. It is a multi-user facility, providing a white neutron source with a neutron energy range from 10 meV to 20 MeV. Up to 10 experiments can be performed simultaneously at measurement stations located between 10 m to 400 m from the neutron production target. The electron linear accelerator provides a pulsed electron beam with a maximum energy of 150 MeV, a peak current of 10 A and a repetition rate ranging from 50 Hz to 800 Hz. A compression magnet reduces the width of the electron pulses to about 2 ns [4]. The electron beam hits a mercury-cooled uranium target producing Bremsstrahlung and subsequently neutrons via photonuclear reactions [5]. Two water-filled beryllium containers mounted above and below the neutron production target are used to moderate the neutrons. By applying different neutron beam collimation conditions, experiments can use either a fast or a thermalized neutron spectrum. The neutron production rate is monitored by BF_3 proportional counters which are mounted in the ceiling of the target hall. The output of the monitors is used to normalize the time-of-flight spectra to the same neutron intensity. The measurement stations are equipped with air conditioning to reduce electronic drifts in the detection chains due to temperature changes.

In this report results of capture cross section measurements carried out at GELINA with three ^{238}U metal samples are described. To reduce bias effects due to e.g. dead time and background, the measurement and data reduction procedures recommended in Ref. [1] have been followed. The main objective of this report is to provide the information that is required to evaluate cross sections for neutron induced reaction on ^{238}U in the resonance region and to extract nuclear reaction model parameters in a least squares adjustment to the data [1]. In the description of the data the recommendations resulting from a consultant's meeting organized by the Nuclear Data Section of the IAEA are followed [6].

2 Experimental conditions

The measurements reported in this work were performed at a 12.5 and 60 m capture measurement station installed at flight path 5 and 14 of GELINA. These flight paths form an angle of 18° and 9°, respectively, with respect to the normal of the moderator face viewing the flight path. The accelerator was operated at 800 Hz and produced an average beam current of about 55 μA. A shadow bar made of Cu and Pb was placed close to the uranium target to reduce the intensity of both the γ-ray flash and the fast neutron component. The moderated neutron beam at the two stations was collimated to about 75 mm in diameter at the sample position. The collimation system was mainly composed of ^{nat}Li and B_4C mixed with epoxy resin, H_3BO_3 mixed with wax, Cu- and Pb-collimators. To minimize the influence of nearby flight paths, shielding walls were built around the detectors. To minimize the contribution of neutrons from a previous burst ^{10}B overlap filters, with an areal density of about 5 x 10^{-3} at/b and about 4.2 x 10^{-2} at/b for the measurements at the 12.5 m and 60 m station, respectively, were placed in the beam. For the measurements at the 12.5 station an 8 mm thick Pb-filter was used to reduce the intensity of the γ-ray flash. Permanent black resonance filters (Na and/or S) were used to monitor the background during the ^{238}U measurements and reduce bias effects related to background corrections. Due to the use of a Na background filter the data in the energy region between 2.5 keV and 3.5 keV cannot be analysed, while the use of a S filter restricts the analysis of the data to an upper limit of 90 keV. Air-conditioning systems are installed in the measurement stations to keep the samples at a constant temperature of about 22°C and to avoid electronic drifts due to temperature changes. The temperature at the sample position was continuously monitored.

The detection systems (i.e. γ-ray detectors, neutron flux detector, electronics and data acquisition system) at the two stations were very similar. Prompt γ-rays originating from neutron induced capture events were detected by a set of C_6D_6–based liquid scintillators (NE230) of 10 cm diameter and 7.5 cm length. The detection system at the 12.5 m station consisted of two detectors and the one at the 60 m station consisted of 4 detectors. Each C_6D_6 detector was positioned at an angle of 125° with respect to the direction of the neutron beam to reduce effects caused by the anisotropy of the dipole radiation. Such a geometry strongly reduces the contribution of in-beam γ–rays to the background. The detection of neutrons scattered from the sample was reduced by coupling each scintillator to a boron-free quartz windowed EMI9823-KQB photomultiplier (PMT). The output signals of the detector were connected to conventional analog electronics. The anode pulse of the PMT was fed into a constant fraction discriminator to create a fast logic signal which defines the arrival time of the neutron creating the capture event in the sample. The signal of the 9th dynode was shaped by a spectroscopic amplifier to determine the energy deposited by the detected γ-rays in the detector. This energy was used to apply weighting function (see section 3). To transfer the observed light output of the scintillators, recorded in channels, into an electron equivalent light output, expressed in energy units, calibration measurements with radionuclide γ-ray sources (^{137}Cs (661 keV), ^{232}Th (2.6 MeV), AmBe (4.4 MeV) and PuC (6.1 MeV)) were carried out. The stability of the C_6D_6 detectors was monitored twice a week by measurements of the 2.6 MeV γ-ray from the ^{232}Th decay chain. The discrimination level of the capture detection system was set to 200 keV deposited energy. This corresponds to the Compton edge of a 330 keV γ-ray.

In the calculation of the weighting function the γ-rays were supposed to be distributed homogenously in the sample and the discrimination level of the detection system was taken into account, as discussed in Ref. [7]. However, this assumption is not valid for the strong resonances. Therefore, a procedure proposed in Refs. [1][8] and implemented in REFIT [9] was applied. The correction factor to account for the γ-ray and neutron transport in the sample was obtained from Monte Carlo simulations using the MCNP 4C2 code [10] and the prompt γ-ray spectrum in the MCNP 4C2 library. The experimental capture yields stored in EXFOR have been corrected for this effect.

The energy dependence of the neutron flux was measured in parallel with ^{10}B-loaded Frisch-gridded ionisation chambers placed at about 80 cm distance before the sample. They were operated with a continuous flow of a mixture of argon (90 %) and methane (10 %) at atmospheric pressure. At the 12.5 m station a double chamber was used with a common cathode loaded with two layers of ^{10}B. The ^{10}B layers with an effective diameter of about 84 mm and areal number density of about 2.1 x 10^{-6} at/b, were evaporated back-to-back on a 30 µm thick aluminium backing and the entrance and exit windows of the chamber had a thickness of 40 µm. The chamber installed at the 60 m station consisted of three back-to-back layers of ^{10}B with a total areal number density of 1.3 x 10^{-5} at/b. The impact of kinematic effects for the flux measurements was strongly reduced by using multiple chambers with a common cathode loaded with two layers of ^{10}B. Such back-to-back configuration, together with an energy threshold on the amplitude spectrum accepting the signals from both the ^{7}Li and the α particles strongly reduces a possible bias related to the forward-to-backward emission ratio [11].

The processing of the time and amplitude signals for the capture and flux detection systems were based on analog electronics. Each system produced a veto signal that created a fixed dead time as soon as a time signal was produced. This fixed dead time was determined by a measurement of the time-interval distribution of successive events. The dead time for the capture detection systems was 2800 ns. Only data for which the dead time correction was less than 20 % were analysed. For the flux measurements the dead time was 3500 ns, with a maximum dead time correction less than 1 %. The dead time corrections for such a system are well understood as demonstrated in Refs. [1][12]. However, it limits the upper energy region of the data obtained at the 12 m station to 70 keV for measurements without the sulfur permanent filter. The presence of the sulfur strongly reduces the impact of the γ-ray flash and its contribution to the dead time correction.

The TOF of a neutron was determined by the time difference between the start signal (T_0), given at each electron burst, and the stop signal (T_s) either from the ^{10}B-chamber or from the C_6D_6 detectors. It was measured with a multi-hit fast time coder with a 1.0 ns resolution, developed at the JRC Geel [13]. The combined time response of the pulsed electron beam and C_6D_6 detection system, including time coder, was verified by a measurement of the γ-ray flash. This resolution can be approximated by a normal distribution with a FHWM of about 2.5 ns. The time response of the ionization chamber was derived from a shape analysis of the transmission dips due to the presence of the sulphur filter. These dips were reproduced supposing a normal distribution with a FWHM of about 40 ns for the time response of the ionization chamber.

The TOF and the pulse height of the capture and flux detection system were independently recorded in list mode using a data acquisition system developed at the JRC Geel [14], allowing for a continuous stability check of the detection systems and an off-line application of the weighting function. The stability of the two detection systems and the accelerator operating conditions (i.e. frequency, current and neutron output) were verified in cycles of 900 seconds. Only cycles with an 800 Hz operating frequency and for which the total neutron intensity and response of the detection systems deviated by less than 2.5 % from the average were selected.

Capture cross section data for ^{238}U were derived from results of measurements using metallic uranium samples. Their characteristics are summarized in Table 1. Two metallic samples, denoted by (1) and (2) in Table 1, were used. They originated from the same batch of uranium material which was enriched to 99.99% in ^{238}U. The isotopic composition of this batch was verified by mass spectrometry in 1984 and resulted in: ^{234}U < 1 ppm, ^{235}U < 11 ppm and ^{236}U < 1 ppm. The areal density of the two samples was derived from a measurement of the mass and the area. The area was determined by an optical surface inspection with a microscopic based measurement system from Mitutoyo (Quick-Scope QS200Z) [15]. The mass of the sample was determined before and after each measurement campaign. Before and after each measurement the surface of each sample was cleaned with cleanroom wipes and methanol to remove possible

oxidation layers. This explains the differences in mass values in Table 1. A conservative uncertainty on the areal density of about 0.25 % was used for the analysis.

Measurements with two different sample geometries (configuration I and configurations II, III in Table 1) and different permanent background filters were carried out. Apart from measurements with the ^{238}U samples, the experimental campaign included additional runs using a ^{208}Pb sample, natural lead samples and only the sample holder. For all ^{238}U and ^{nat}Pb sample geometries the area of the neutron beam at the sample position (~ 38 cm^2) was larger than the effective sample area. During a first campaign at 12.5 m, the two ^{238}U samples were placed in a back-to-back geometry resulting in a 12.2 g sample with nominal dimensions (54 mm x 30 mm x 0.46 mm) and an areal number density of (1.920 ± 0.005) x 10^{-3} at/b. The measurements with this sample geometry denoted by configuration I in Table 1, were carried out with permanent Na and S filters in the beam. In a second campaign at 12.5 m the two samples were combined to form a 12.1 g sample with nominal dimensions (53 mm x 60 mm x 0.23 mm) and an areal number density of (0.9530 ± 0.0025) x 10^{-3} at/b (configuration III in Table 1). During these measurements only the Na filter was used as permanent background filter. A similar sample geometry was used for the measurements at the 60 m station (configuration II in Table 1). For these measurements the areal number density of the ^{238}U sample was (0.9554 ± 0.0025) x 10^{-3} at/b and only the S filter was used as a permanent background filter.

Sample	Shape	Area/cm^2	Mass/g	Areal Density (at/b)	Station (filters)
^{238}U (1I)	foil	15.94 ± 0.01	6.030 ± 0.015	(9.570 ± 0.025) x 10^{-4}	12.5 m (S, Na)
^{238}U (2I)	foil	16.21 ± 0.01	6.170 ± 0.015	(9.628 ± 0.025) x 10^{-4}	12.5 m (S, Na)
^{238}U (1II)	foil	15.94 ± 0.01	6.009 ± 0.015	(9.536 ± 0.025) x 10^{-4}	60 m (S)
^{238}U (2II)	foil	16.21 ± 0.01	6.134 ± 0.015	(9.572 ± 0.025) x 10^{-4}	60 m (S)
^{238}U (1III)	foil	15.94 ± 0.01	6.000 ± 0.015	(9.522 ± 0.025) x 10^{-4}	12.5 m (Na)
^{238}U (2III)	foil	16.21 ± 0.01	6.112 ± 0.015	(9.537 ± 0.025) x 10^{-4}	12.5 m (Na)
^{nat}Pb (1)	foil	15.89 ± 0.01	9.264 ± 0.001	(1.694 ± 0.001) x 10^{-3}	
^{nat}Pb (2)	foil	16.23 ± 0.01	9.442 ± 0.001	(1.691 ± 0.001) x 10^{-3}	
^{208}Pb	disc	50.27 ± 0.01	29.732 ± 0.001	(1.713 ± 0.001) x 10^{-3}	

Table 1 Characteristics of the samples used for the capture measurements performed at GELINA. The masses for the different configurations of the samples (denoted by configurations I, II and III) change due to the removal of the oxidation before each measurement campaign. The different sample configurations consisted of two metallic foils, which are denoted by 1 and 2.

3 Data reduction

The total energy detection principle combined with the pulse height weighting technique was applied to make the detection efficiency for a capture event directly proportional to the total γ-ray energy available in the capture event [1][7]. The list mode data were sorted into TOF-histograms after verification of the stability of the detection systems. Each event recorded in the C_6D_6 detectors was weighted using a weighting function which was determined by Monte Carlo simulations as described in Ref. [7]. In the calculation of the weighting function the effect of the discrimination level was taken into account. To account for neutron and γ-ray transport in the sample the procedure described in Refs. [1][8] was applied. The γ-rays were assumed to be homogeneously distributed in the sample and a correction factor to account for the non-homogeneous distribution of the γ-rays due to the attenuation of the neutron beam in the sample was applied.

3.1 Experimental capture yield

The experimental yield Y_{exp} was derived from the ratio of the observed response of the capture detection system and the response of the neutron flux detector [1]:

$$Y_{exp} = \frac{N_c}{S_n + E_n \frac{A}{1+A}} F_c \frac{C_w - B_w}{C_\varphi - B_\varphi} \frac{Y_\varphi}{T_\varphi}, \tag{3.1}$$

where E_n is the kinetic energy of the neutron, S_n is the neutron separation energy and A is the mass number of the target nucleus. The dead time corrected weighted response of the C_6D_6 detection system is denoted by C_w and its background contribution by B_w. The dead time corrected TOF-spectrum resulting from the flux measurements is C_φ and its background contribution is B_φ. All spectra are normalized to the same neutron intensity. The quantity Y_φ/T_φ , dependent equivalently on TOF or energy, is given by:

$$\frac{Y_\varphi}{T_\varphi} = e^{n\sigma_{tot}}(1 - e^{-n\sigma_{tot}}) \frac{\sigma_\alpha}{\sigma_{tot}}, \tag{3.2}$$

where σ_{tot} and σ_α are the $^{10}B(n,tot)$ and $^{10}B(n,\alpha)$ cross sections, respectively, and n is the total areal number density of the ^{10}B layers in the ionisation chamber. Before applying Eq. (3.2) a transformation of variables was applied to account for the ~80 cm difference in the position of the ionization chamber and the capture sample. The normalization factor N_c accounts for energy-independent factors, such as the effective sample area seen by the neutron beam, the efficiency of the flux detector and the solid angle subtended by the sample and the C_6D_6 detectors.

The time-of-flight t of a neutron creating a signal in the neutron detector was determined by the time difference between the start signal (T_0) and the stop signal (T_s):

$$t = (T_s - T_0) + t_0, \tag{3.3}$$

with t_0 a time-offset which was determined by a measurement of the γ-ray flash.

3.2 Background for the flux measurements

The background contribution for the flux measurements was approximated by an analytical function applying the black resonance technique [1]. The analytical function was a sum of a time independent and two time dependent components:

$$B_\varphi(t) = K_\varphi\left[a_0 + a_1 e^{-\lambda_1 t} + a_2 e^{-\lambda_2 (t+\tau_0)}\right], \tag{3.4}$$

where *t* denotes the TOF of the detected event. The analytical expression and decay constants λ_1 and λ_2 were derived from additional measurements with Ag, W, Co, Na and S black resonance filters and measurements at lower operating frequency. The time independent component a_0 accounts for ambient background and scattered neutrons which are produced in the target room but which have completely lost their time correlation with the pulsed electron beam. The first time-dependent component accounts for neutrons that are scattered inside the detector station and for neutrons scattered at other flight paths. The second time-dependent component corresponds to the contribution due to slow neutrons from previous accelerator pulses. This contribution was estimated by an extrapolation of the TOF-spectrum at the end of the cycle. It is approximated by an exponential decay, where the parameter τ_0 is equal to the spacing between the electron bursts. For an operating frequency of 800 Hz, τ_0 = 1.25 ms. The factor K_φ = 1.00 ± 0.03 is introduced in Eq. (3.4) to account for uncertainties due to systematic effects in the background correction. This parameter, which is valid for the measurements at 12.5 m and 60 m, was obtained from results of a series of additional measurements with Ag, W, Co, Na and S black resonance filters in the beam. The parameter together with its uncertainty was derived from a statistical analysis of the difference between observed black resonance dips and the background estimated by the analytical expression in Eq. (3.4).

3.3 Background for the capture measurements

The total background contribution to the weighted response of the C_6D_6 detectors was expressed as:

$$B_w(t) = K_\gamma \left[b_0 + C_{w,0}(t) + R_n(t) \left(C_{w,Pb}(t) - C_{w,0}(t) \right) \right], \tag{3.5}$$

where b_0 is a time independent contribution, $C_{w,0}$ and $C_{w,Pb}$ are the weighted TOF-spectra from measurements with no sample and with an almost purely scattering ^{208}Pb sample, respectively. The weighted spectra $C_{w,0}$ and $C_{w,Pb}$, corrected for the time independent background, were derived with the weighting function for the ^{238}U sample and normalized to the same integrated neutron intensity.

To account for the different geometry of the ^{238}U and ^{208}Pb samples (see Table 1), the ^{208}Pb spectra were normalised to the ^{nat}Pb spectra in regions where no resonance contributions from ^{204,206,207}Pb were observed. The correction factor R_n is the ratio of the neutron scattering yield of the U and Pb sample. This factor, which is expressed as a function of TOF, was derived from Monte Carlo simulations using the MCNP 4C2 code.

The factor K_γ = 1.00 ± 0.03, which is introduced to account for the uncertainty due to systematic effects in the background correction, was obtained from a systematic study of the background based on Eq. (3.5) and the background dips present in the TOF-spectra due to the presence of black resonances filters.

The contribution of prompt fission γ-rays from ^{238}U(n,f) to the weighted response was estimated using a prompt γ-ray spectrum for ^{238}U(n,f) of Litaize et al. [16] and an average total prompt γ-ray energy of (6.7 ± 0.5) MeV. The prompt fission and capture γ-ray spectra were supposed to be independent of incoming neutron energy. The ratio of weighted detection efficiency for a fission event and capture event was estimated to be 0.6 ± 0.3. Due to the low contribution of this background component, a conservative estimate of the relative uncertainty of this ratio is the relative standard deviation of the total prompt fission γ-ray energy distribution. This standard deviation is about 3.5 MeV. For the 726 eV resonance, for which the largest fission-to-capture ratio is reported, the relative contribution due to prompt fission γ-rays is less than 5%. In the other energy regions of interest the contribution is less than 0.5%.

3.4 Correction factor F_c

The relation between the average capture cross section $\overline{\sigma}_\gamma$ and average experimental yield $\overline{Y}_{exp}$, expressing the probability that a neutron creates a capture event in the sample, is mostly expressed as []:

$$\overline{Y}_{exp} = F_c n \overline{\sigma}_\gamma, \tag{3.3}$$

Where n is the areal number density and F_c is an energy-dependent factor to correct for self-shielding and multiple interaction event, i.e. neutron scattering followed by neutron capture. This factor was calculated by Monte Carlo simulations using the MCNP 4C2 code applying probability tables to produce resonance structured cross sections in the URR. These tables were created by NJOY []. The correction factor for the two sample geometries are compared n Fig.1. The structures at 35 keV and 90 keV are due to the presence of the aluminium foil around the sample. For relatively thin samples, as those used in this work, the uncertainty on this correction factor is ≤ 0.5 % as demonstrated in Ref. [].

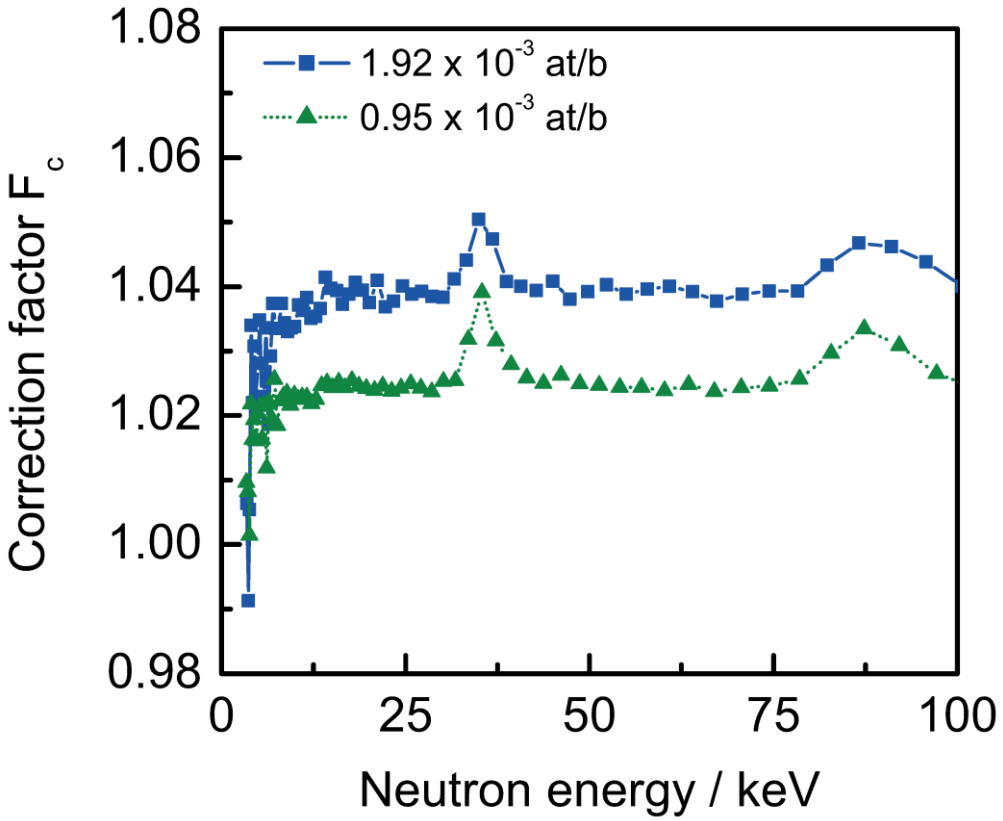

Figure 1 Correction factor Fc to account for self-shielding and multiple interaction events as a function of the neutron energy. The factor is shown for the two sample geometries discussed in sect. 2.2 and specified in table 1.

3.5 Normalization

The experimental yields resulting from the measurements at 12.5 m, obtained with the two sample geometries (I and III), were internally normalised using the profile of the well-isolated and saturated resonance at 6.67 eV. This resonance has a low scattering to capture ratio of about 0.06. The normalisation was obtained by a least squares adjustment of the experimental yield with only the normalization factor as a free fitting parameter. Only data points close to the resonance top, with a yield $\geq$ 0.75, were considered in the fit. Using a saturated profile from a resonance with a neutron width that is much smaller than the radiation width results in a normalisation that is nearly independent of the resonance parameters and sample thickness [1]. If, in addition, an internal normalization is applied, most of the experimental conditions remain unchanged and a bias due to systematic effects, such as variations of detector and accelerator operating conditions, effective sample area seen by the neutron beam, solid angle between sample and detector, is nearly eliminated [1]. The normalisation factor for the capture data obtained at 60 m was derived from a simultaneous resonance shape analysis including the 12.5 m capture data shown in **Error! Reference source not found.** and the transmission data of Olsen et al. [17][18]. Only data in the energy region between 150 eV and 300 eV were included in this analysis.

3.6 Time–of–flight to energy conversion

The zero point of the time scale for the capture detection system was deduced from the position of the γ-ray flash with an accuracy better than 1 ns. A resonance shape analysis of ^{238}U(n,γ) resonances below 500 eV was used to define the effective flight path length using the resonance energies of Derrien et al. [19]. The flight path lengths were (12.942 ± 0.002) m and (12.964 ± 0.002) m for the measurements with the (1.92×10^{-3}) at/b and (0.953×10^{-4}) at/b samples, respectively. For the measurements with sample configuration II the flight path length was (58.580 ± 0.005) m. These distances are from the centre of the moderator to the centre of the sample. The quoted uncertainties are only due to the propagation of counting statistics uncertainties and do not account for uncertainties on the resonance energies. The zero point of the time scale for the flux system was derived from dips in the TOF-spectrum due to Pb resonances. The flight path length was derived from resonance dips in the TOF-spectra obtained from measurements with the W and Ag filters in the beam.

4 Results

To derive the experimental yield and propagate both the correlated and uncorrelated uncertainties the AGS code was used [20]. The AGS (Analysis Of Geel Spectra) code, developed at the EC-JRC, was used to derive the experimental yield. The code is based on a compact formalism to propagate all uncertainties starting from uncorrelated uncertainties due to counting statistics. It stores the full covariance information after each operation in a concise, vectorized way. The AGS formalism results in a substantial reduction of data storage volume and provides a convenient structure to verify the various sources of uncertainties through each step of the data reduction process. The concept is recommended by the Nuclear Data Section of the IAEA [6] to prepare the experimental observables, including their full covariance information, for storage into the EXFOR data library [21][22].

The format in which the numerical data will be stored in the EXFOR data library is illustrated in Tables B.1, B.2 and B.3 in the Appendix. The data include the full covariance information based on the AGS concept. The total uncertainty and the uncertainty due to uncorrelated components are reported, together with the contributions due to the normalization and background subtraction. Applying the AGS concept described in Ref. [20], the covariance matrix V of the experimental transmission can be calculated by:

$$V = U_u + S(\eta)S(\eta)^T, \tag{4.1}$$

where U_u is a diagonal matrix containing the contribution of all uncorrelated uncertainty components. The matrix S is contains the contribution of the components η = {N, K_γ, K_φ} creating correlated components. The uncertainty due to the dead time correction can be neglected.

The experimental details, which are required to perform a resonance analysis on the data, are summarized in Appendix A1, A2 and A3. The information given is based on the recommendations resulting from a consultant's meeting organized by the NDS-IAEA [6].

References

[1] P. Schillebeeckx, B. Becker,Y. Danon, K. Guber, H. Harada, J. Heyse, A.R. Junghans, S. Kopecky, C. Massimi, M.C. Moxon, N. Otuka, I. Sirakov and K. Volev, "Determination of resonance parameters and their covariances from neutron induced reaction cross section data", Nucl. Data Sheets 113 (2012) 3054 – 3100.

[2] A. Bensussan and J.M. Salomé, "GELINA: A modern accelerator for high resolution neutron time of flight experiments", Nucl. Instr. Meth. 155 (1978) 11 – 23.

[3] W. Mondelaers and P. Schillebeeckx, "GELINA, a neutron time-of-flight facility for neutron data measurements", Notiziario Neutroni e Luce di Sincrotrone 11 (2006) 19 – 25.

[4] D. Tronc, J.M. Salomé and K.H. Böckhoff, "A new pulse compression system for intense relativistic electron beams", Nucl. Instr. Meth. 228 (1985) 217 – 227.

[5] J.M. Salome and R. Cools, "Neutron producing targets at GELINA", Nucl. Instr. Meth. 179 (1981) 13 – 19.

[6] F. Gunsing, P. Schillebeeeckx and V. Semkova, Summary Report of the Consultants' Meeting on EXFOR Data in Resonance Region and Spectrometer Response Function, IAEA Headquarters, Vienna, Austria, 8-10 October 2013, INDC(NDS)-0647 (2013), https://www-nds.iaea.org/index-meeting-crp/CM-RF-2013/ (03/05/2016).

[7] A. Borella, G. Aerts, F. Gunsing, M. Moxon, P. Schillebeeckx and R. Wynants, "The use of C_6D_6 detectors for neutron induced capture cross-section measurements in the resonance region", Nucl. Instr. Meth. A 577 (2007) 626.

[8] P. Schillebeeckx, A. Borella, S. Kopecky, C. Lampoudis, C. Massimi and M. Moxon, "Neutron Resonance Spectroscopy at GELINA", J. Korean Phys. Soc. 59 (2011) 1563.

[9] M.C. Moxon and J.B. Brisland, Technical Report AEA-INTEC-0630, AEA Technology (1991).

[10] J. Briemeister, MCNP, A General Monte Carlo N-Particle Transport Code, Version 4C2, in LA-13709-M (2000).

[11] G. Giorginis and V. Khriatchkov, "The effect of particle leaking and its implications for measurements of the (n,α) reaction on light elements by using ionisation chambers", Nucl. Instr. Meth. A 538 (2005) 550 – 558.

[12] L.C. Mihailescu, A. Borella, C. Massimi and P. Schillebeeckx, "Investigations for the use of the fast digitizers with C6D6 detectors for radiative capture measurements at GELINA", Nucl. Instr. Meth. A 600 (2009) 453 – 459.

[13] S. de Jonge, "Fast Time Digitizer Type 8514 A", Internal Report GE/DE/R/24/87, IRMM, Geel

[14] J. Gonzalez, C. Bastian, S. de Jonge, and K. Hofmans, "Modular Multi-Parameter Multiplexer MMPM. Hardware description and user guide", Internal Report GE/R/INF/06/97, IRMM, Geel.

[15] https://www.mitutoyo.co.jp/eng/ (03/06/2016).

[16] O.Litaize, O. Serot, D. Regnier and C. Manailescu, "Investigation of n+^{238}U Fission Observables", Nucl. Data Sheets 118 (2014) 216.

[17] D.K. Olsen, G. de Saussure, R.B. Perez, E.G. Silver, F.C. Difilippo, R.W. Ingle and H. Weaver, "Precise Measurement and Analysis of Neutron Transmission Through Uranium-238", Nucl. Sci. Eng. 62 (1977) 479 - 501.

[18] D.K. Olsen, G. de Saussure, R.B. Perez, F.C. Difilippo and R.W. Ingle, "Note on ^{238}U+n Resolved Resonances Energies", Nucl. Sci. Eng. 66 (1978) 141 - 144.

[19] H. Derrien, L.C. Leal, N.M. Larson and A. Courcelle, "Neutron Resonance Parameters and Calculated Cross Sections from Reich-Moore Analysis of Experimental Data in the Neutron Energy Range from 0 to 20 keV", ORNL/TM-2005/241, Oak Ridge National Laboratory, (2005).

[20] B. Becker, C. Bastian, F. Emiliani, F. Gunsing, J. Heyse, K. Kauwenberghs, S. Kopecky, C. Lampoudis, C. Massimi, N. Otuka, P. Schillebeeckx and I. Sirakov, "Data reduction and uncertainty propagation of time-of-flight spectra with AGS", J. of Instrumentation, 7 (2012) P11002 – 19.

[21] N. Otuka, A. Borella, S. Kopecky, C. Lampoudis, and P. Schillebeeckx, "Database for time-of-flight spectra with their covariances", J. Korean Phys. Soc. 59 (2011) 1314 – 1317.

[22] N. Otuka, S. Dunaeva, E. Dupont, O. Schwerer and A. Blokhin, "The role of the nuclear reaction data centres in experimental nuclear data knowledge sharing", J. Korean Phys. Soc. 59 (2011) 1292 – 1297.

List of figures

Figure 1 Correction factor Fc to account for self-shielding and multiple interaction events as a function of the neutron energy. The factor is shown for the two sample geometries discussed in sect. 2.2 and specified in table 1. 13

List of tables

Table 1 Characteristics of the samples used for the capture measurements performed at GELINA. The masses for the different configurations of the samples (denoted by configurations I, II and III) change due to the removal of the oxidation before each measurement campaign. The different sample configurations consisted of two metallic foils, which are denoted by 1 and 2. 10

Appendix

A. SUMMARY OF EXPERIMENTAL DETAILS

A. 1 Experiment description (CONFIG. I)

1.	**Main Reference**		[1][2]
2.	**Facility**	GELINA	[3]
3.	**Neutron production**		
	Neutron production beam	Electron	
	Nominal average beam energy	100 MeV	
	Nominal beam power (peak current)	10 A	
	Repetition rate (pulses per second)	800 Hz	
	Pulse width	1 ns	
	Primary neutron production target	Mercury cooled depleted uranium	
	Target nominal neutron production intensity	3.4×10^{13} s^{-1}	
4.	**Moderator**		
	Primary neutron source position in moderator	Above and below uranium target	
	Moderator material	2 water filled Be-containers around U-target	
	Moderator dimensions (internal)	2 x (14.6 cm x 21 cm x 3.9 cm)	
	Density (moderator material)	1 g/cm^2	
	Temperature (K)	Room temperature	
	Moderator-room decoupler (Cd, B, …)	None	
5.	**Other experimental details**		
	Measurement type	Capture	
	Method (total energy, total absorption, …)	Total energy + Pulse Height Weighting	[4][5]
	Flight Path length (m) (moderator centre– detector front face)	L = (12.942 ± 0.002) m	
	Flight path direction	18° with respect to normal of the moderator face viewing the flight path	
	Neutron beam dimensions at sample position	75 mm in diameter	
	Neutron beam profile	-	
	Overlap suppression	^{10}B overlap filter (5×10^{-3} at/b)	
	Other fixed beam filters	S, Na	
6.	**Detector**		
	Type	Scintillator (NE230)	
	Material	2 x C_6D_6 (coupled to PMT by quartz window)	
	Surface Dimensions	10 cm diameter	
	Thickness (cm)	7.5 cm	
	Distance from samples (cm)	10 cm	
	Detector(s) position relative to neutron beam	125°	
	Detector(s) solid angle	-	
7.	**Sample**		
	Type (metal, powder, liquid, crystal)	Metal	
	Chemical composition	^{238}U (99.99 %: ^{234}U<1ppm, ^{235}U<11ppm, ^{236}U<1ppm)	
	Sample composition (at/b)	^{238}U (1.920 ± 0.005) x 10^{-3} at/b	

	Temperature	22 ℃	
	Sample mass (g)	(12.200 ± 0.03) g	
	Geometrical shape (cylinder, sphere, …)	Foil (rectangular)	
	Surface dimension	54 mm x 30 mm	
	Nominal thickness (mm)	0.46 mm	
	Containment description	Al container	
	Additional comment	Sample composed by two individual samples	
8.	**Data Reduction Procedure**		[5][6]
	Dead time correction	Done (< factor 1.2)	
	Back ground subtraction	Capture: including neutron sensitivity	
	Flux determination (reference reaction, …)	$^{10}B(n,\alpha)$	
	Normalization	1.000 ± 0.015	
	Detector efficiency	-	
	Self-shielding	-	
	Time-of-flight binning	Zone length bin width 7168 1 ns 4096 2 ns 4096 4 ns 4096 8 ns 4096 16 ns 3072 32 ns 3072 64 ns 4096 128 ns 9216 256 ns 2048 8192 ns	
9.	**Response function**		
	Initial pulse	Normal distribution, FWHM = 2 ns	
	Target / moderator assembly	Numerical distribution from MC simulations	[7][8]
	Detector	Analytical function defined in REFIT manual	[9]

A. 2 Experiment description (CONFIG. II)

1.	**Main Reference**		[1][2]
2.	**Facility**	GELINA	[3]
3.	**Neutron production**		
	Neutron production beam	Electron	
	Nominal average beam energy	100 MeV	
	Nominal beam power (peak current)	10 A	
	Repetition rate (pulses per second)	800 Hz	
	Pulse width	1 ns	
	Primary neutron production target	Mercury cooled depleted uranium	
	Target nominal neutron production intensity	3.4 $x10^{13}$ s^{-1}	
4.	**Moderator**		
	Primary neutron source position in moderator	Above and below uranium target	
	Moderator material	2 water filled Be-containers around U-target	
	Moderator dimensions (internal)	2 x (14.6 cm x 21 cm x 3.9 cm)	
	Density (moderator material)	1 g/cm^2	

	Temperature (K)	Room temperature	
	Moderator-room decoupler (Cd, B, …)	None	
5.	**Other experimental details**		
	Measurement type	Capture	
	Method (total energy, total absorption, …)	Total energy + Pulse Height Weighting	[4][5]
	Flight Path length (m) (moderator centre – detector front face)	L = (58.580 ± 0.005) m	
	Flight path direction	9° with respect to normal of the moderator face viewing the flight path	
	Neutron beam dimensions at sample position	75 mm in diameter	
	Neutron beam profile	-	
	Overlap suppression	^{10}B overlap filter (4.2x10^{-2} at/b)	
	Other fixed beam filters	S	
6.	**Detector**		
	Type	Scintillator (NE230)	
	Material	4 x C_6D_6 (coupled to PMT by quartz window)	
	Surface Dimensions	10 cm	
	Thickness (cm)	7.5 cm in thick	
	Distance from samples (cm)	10 cm	
	Detector(s) position relative to neutron beam	125°	
	Detector(s) solid angle	-	
7.	**Sample**		
	Type (metal, powder, liquid, crystal)	Metal	
	Chemical composition	^{238}U (99.99 %: ^{234}U<1ppm, ^{235}U<11ppm, ^{236}U<1ppm)	
	Sample composition (at/b)	^{238}U: (0.9554 ± 0.0025) 10^{-3} at/b	
	Temperature	22 ℃	
	Sample mass (g)	(12.143 ± 0.03) g	
	Geometrical shape (cylinder, sphere, …)	Foil (rectangular)	
	Surface dimension	54 mm x 60 mm	
	Nominal thickness (mm)	0.23 mm	
	Containment description	Al container	
	Additional comment	Sample composed by two individual samples	
8.	**Data Reduction Procedure**		[5][6]
	Dead time correction	Done (< factor 1.2)	
	Back ground subtraction	Capture: including neutron sensitivity	
	Flux determination (reference reaction, …)	^{10}B(n,α)	
	Normalization	1.000 ± 0.015	
	Detector efficiency	-	
	Self-shielding	-	
	Time-of-flight binning	Zone length bin width 20480 1 ns 3072 32 ns 3072 64 ns 3072 128 ns 3072 256 ns 4096 16384 ns	
9.	**Response function**		
	Initial pulse	Normal distribution, FWHM = 2 ns	
	Target / moderator assembly	Numerical distribution from MC	[7][8]

	simulations	
Detector	Analytical function defined in REFIT manual	[9]

A. 3 Experiment description (CONFIG. III)

1. Main Reference		[1][2]
2. Facility	GELINA	[3]
3. Neutron production		
Neutron production beam	Electron	
Nominal average beam energy	100 MeV	
Nominal beam power (peak current)	10 A	
Repetition rate (pulses per second)	800 Hz	
Pulse width	1 ns	
Primary neutron production target	Mercury cooled depleted uranium	
Target nominal neutron production intensity	3.4 x10^{13} s^{-1}	
4. Moderator		
Primary neutron source position in moderator	Above and below uranium target	
Moderator material	2 water filled Be-containers around U-target	
Moderator dimensions (internal)	2 x (14.6 cm x 21 cm x 3.9 cm)	
Density (moderator material)	1 g/cm^2	
Temperature (K)	Room temperature	
Moderator-room decoupler (Cd, B, …)	None	
5. Other experimental details		
Measurement type	Capture	
Method (total energy, total absorption, …)	Total energy + Pulse Height Weighting	[4][5]
Flight Path length (m) (moderator centre – detector front face)	L = (12.964 ± 0.002) m	
Flight path direction	18° with respect to normal of the moderator face viewing the flight path	
Neutron beam dimensions at sample position	75 mm in diameter	
Neutron beam profile	-	
Overlap suppression	^{10}B overlap filter (5x10^{-3} at/b)	
Other fixed beam filters	Na	
6. Detector		
Type	Scintillator (NE230)	
Material	2 x C_6D_6 (coupled to PMT by quartz window)	
Surface Dimensions	10 cm diameter	
Thickness (cm)	7.5 cm in thick	
Distance from samples (cm)	10 cm	
Detector(s) position relative to neutron beam	125°	
Detector(s) solid angle	-	
7. Sample		
Type (metal, powder, liquid, crystal)	Metal	
Chemical composition	^{238}U (99.99 %: ^{234}U<1ppm, ^{235}U<11ppm, ^{236}U<1ppm)	
Sample composition (at/b)	^{238}U: (0.9530 ± 0.0025) 10^{-3} at/b	

Temperature	22 ℃	
Sample mass (g)	(12.112 ± 0.03) g	
Geometrical shape (cylinder, sphere, …)	Foil (rectangular)	
Surface dimension	54 mm x 60 mm	
Nominal thickness (mm)	0.23 mm	
Containment description	Al container	
Additional comment	Sample composed by two individual samples	
8. Data Reduction Procedure		[5][6]
Dead time correction	Done (< factor 1.2)	
Back ground subtraction	Capture: including neutron sensitivity	
Flux determination (reference reaction, …)	$^{10}B(n,\alpha)$	
Normalization	1.000 ± 0.015	
Detector efficiency	-	
Self-shielding	-	
Time-of-flight binning	Zone length bin width 1024 16 ns 11264 1 ns 10240 2 ns 5120 8 ns 4096 32 ns 4096 128 ns 1024 16384 ns	
9. Response function		
Initial pulse	Normal distribution, FWHM = 2 ns	
Target / moderator assembly	Numerical distribution from MC simulations	[7][8]
Detector	Analytical function defined in REFIT manual	[9]

B. Data format

Column	Content	Unit	Comment
1	E_l	eV	Energy of lower bound
2	E_h	eV	Energy of upper bound
3	$\bar{\sigma}_\gamma$		Capture yield
4	Total Uncertainty		
5	Uncorrelated uncertainty		Uncorrelated uncertainty due to counting statistics
6	AGS-vector (K_γ)		Correlated uncertainty due to background of capture ($u_{k\gamma}/K\gamma$ =3 %)
7	AGS-vector (K_φ)		Correlated uncertainty due to background of flux ($u_{k\varphi}/K_\varphi$ = 3 %)
8	AGS-vector (N)		Correlated uncertainty due to Normalization (u_N/N = 1.5 %)

Comments from the authors:

- The AGS concept was used to derive the experimental averaged capture yield in given energy boundary and to propagate the uncertainties, both the uncorrelated due to counting statistics and the uncertainty due to the normalization and the background contributions. Then the averaged capture cross section is obtained as:

$$\overline{\sigma_\gamma} = \frac{1}{F_c}\frac{1}{n}\overline{Y}_{exp},$$

where F_c is correction factor and n is an areal density.

B.1 DATA

E_l/ eV	E_h/ eV	$\bar{\sigma}_\gamma$/b	$u_{\bar{\sigma}_\gamma}$/b	AGS			
				u_u /b	S_{K_c} /b	S_{K_φ} /b	S_{N_c} /b
3500	4000	0.9828	0.0340	0.0138	-0.0273	1.7×10^{-5}	0.0147
4000	4500	0.8645	0.0246	0.0092	-0.0188	1.3×10^{-5}	0.0130
4500	5000	0.9743	0.0234	0.0085	-0.0162	1.2×10^{-5}	0.0146
5000	5500	0.8448	0.0209	0.0080	-0.0146	1.1×10^{-5}	0.0127
5500	6000	0.9355	0.0220	0.0088	-0.0145	1.1×10^{-5}	0.0140
6000	6500	0.9226	0.0212	0.0087	-0.0135	1.1×10^{-5}	0.0138
6500	7000	0.8286	0.0198	0.0085	-0.0129	1.1×10^{-5}	0.0124
7000	8000	0.7726	0.0174	0.0058	-0.0116	1.0×10^{-5}	0.0116
8000	9000	0.6521	0.0153	0.0056	-0.0104	9.7×10^{-6}	0.0098
9000	10000	0.6958	0.0152	0.0054	-0.0096	9.4×10^{-6}	0.0104
10000	12000	0.6657	0.0138	0.0039	-0.0087	9.1×10^{-6}	0.0100
12000	14000	0.6458	0.0132	0.0040	-0.0079	9.1×10^{-6}	0.0097
14000	16000	0.5860	0.0120	0.0040	-0.0071	8.9×10^{-6}	0.0088
16000	18000	0.5787	0.0117	0.0040	-0.0067	8.8×10^{-6}	0.0087
18000	20000	0.5366	0.0108	0.0039	-0.0060	8.5×10^{-6}	0.0081
20000	22500	0.5246	0.0103	0.0035	-0.0056	8.5×10^{-6}	0.0079
22500	25000	0.4871	0.0095	0.0033	-0.0050	8.2×10^{-6}	0.0073
25000	27500	0.4608	0.0090	0.0033	-0.0048	7.5×10^{-6}	0.0069
27500	30000	0.4453	0.0089	0.0035	-0.0047	7.1×10^{-6}	0.0067
30000	35000	0.4230	0.0088	0.0031	-0.0052	7.8×10^{-6}	0.0064
35000	40000	0.3942	0.0077	0.0026	-0.0042	7.2×10^{-6}	0.0059
40000	45000	0.3767	0.0069	0.0022	-0.0033	7.4×10^{-6}	0.0057
45000	50000	0.3457	0.0063	0.0021	-0.0029	8.2×10^{-6}	0.0052
50000	60000	0.2959	0.0055	0.0016	-0.0028	1.1×10^{-5}	0.0044
60000	70000	0.2473	0.0044	0.0013	-0.0021	1.6×10^{-5}	0.0037
70000	80000	0.2093	0.0038	0.0012	-0.0018	9.2×10^{-5}	0.0031
80000	90000	0.1915	0.0040	0.0017	-0.0022	1.4×10^{-4}	0.0029

References

[1] H. I. Kim, C. Paradela, I. Sirakov, B. Becker, R. Capote, F. Gunsing, G.N., Kim, S. Kopecky, C. Lampoudis, Y.-O. Lee, R. Massarczyk, A. Moens, M. Moxon, V.G. Pronyaev, P. Schillebeeckx and R. Wynants, "Neutron capture cross section measurements for ^{238}U in the resonance region at GELINA", Eur. Phys. J. A 52 (2016) 170.

[2] H. I. Kim, C. Paradela, S. Kopecky, G. Alaerts, A. Moens, P. Schillebeeckx and R. Wynants, "Results of capture cross section measurements for ^{238}U at a 12 m and 60 m station of GELINA", EUR xxxxx EN; doi: xx.xxxx/xxxxxx.

[3] W. Mondelaers and P. Schillebeeckx, "GELINA, a neutron time-of-flight facility for neutron data measurements", Notiziario Neutroni e Luce di Sincrotrone, 11 (2006) 19 – 25.

[4] B. Becker, C. Bastian, F. Emiliani, F. Gunsing, J. Heyse, K. Kauwenberghs, S. Kopecky, C. Lampoudis, C. Massimi, N. Otuka, P. Schillebeeckx and I. Sirakov, "Data reduction and uncertainty propagation of time-of-flight spectra with AGS", J. of Instrumentation, 7 (2012) P11002 – 19.

[5] P. Schillebeeckx, B. Becker,Y. Danon, K. Guber, H. Harada, J. Heyse, A.R. Junghans, S. Kopecky, C. Massimi, M.C. Moxon, N. Otuka, I. Sirakov and K. Volev, "Determination of resonance parameters and their covariances from neutron induced reaction cross section data", Nuclear Data Sheets 113 (2012) 3054 – 3100.

[6] B. Becker, C. Bastian, F. Emiliani, F. Gunsing, J. Heyse, K. Kauwenberghs, S. Kopecky, C. Lampoudis, C. Massimi, N. Otuka, P. Schillebeeckx and I. Sirakov, "Data reduction and uncertainty propagation of time-of-flight spectra with AGS", J. of Instrumentation, 7 (2012) P11002 – 19.

[7] M. Flaska, A. Borella, D. Lathouwers, L.C. Mihailescu, W. Mondelaers, A.J.M. Plompen, H. van Dam, T.H.J.J. van der Hagen, "Modeling of the GELINA neutron target using coupled electron–photon–neutron transport with the MCNP4C3 code", Nucl. Instr. Meth. A 531 (2004) 392–406.

[8] D. Ene, C. Borcea, S. Kopecky, W. Mondelaers, A. Negret and A.J.M. Plompen, "Global characterisation of the GELINA facility for high-resolution neutron time-of-light measurements by Monte Carlo simulations", Nucl. Instr. Meth. A 618 (2100) 54 - 68.

[9] M.C. Moxon and J.B. Brisland, Technical Report AEA-INTEC-0630, AEA Technology (1991).

LC-NA-28347-EN-N

JRC Mission

As the Commission's in-house science service, the Joint Research Centre's mission is to provide EU policies with independent, evidence-based scientific and technical support throughout the whole policy cycle.

Working in close cooperation with policy Directorates-General, the JRC addresses key societal challenges while stimulating innovation through developing new methods, tools and standards, and sharing its know-how with the Member States, the scientific community and international partners.

Serving society
Stimulating innovation
Supporting legislation

doi:10.2789/34219

ISBN 978-92-79-64614-0